Supplemental Materials

Online Figure I.

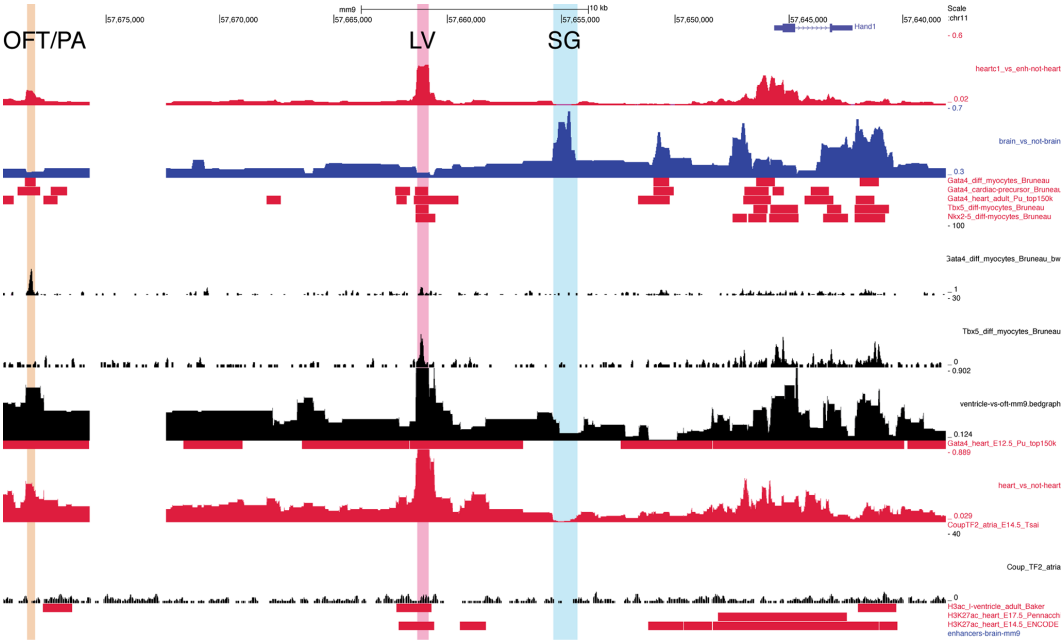

Online Figure I. EMERGE tracks predict GATA4 binding to the predicted *Hand1* cardiac enhancer. The LV enhancer (pink) is predicted to be a cardiac enhancer and is enriched for GATA4 binding in ChIP-Seq datasets. Previously characterized sympathetic ganglia (SG; blue) and outflow tract / pharyngeal arch (OFT/PA; orange) enhancers are also predicted. GATA4 binding to the GATA-dependent outflow tract / pharyngeal arch enhancer has been confirmed .[38] All tracks represent murine sequences.

Online Figure II.

A

Gene	Human coordinates (hg38, chr5)	Mouse coordinates (mm10, chr11)
FAM114A2	153,990,128-154,038,919	57,482,990-57,518,644
MFAP3	154,038,959-154,054,052	57,518,665-57,533,817
GALNT10	154,190,730-154,420,984	57,645,442-57,787,501
SAP30L	154,446,545-154,456,331	57,801,637-57,810,615
HAND1	154,474,972-154,478,264	57,828,713-57,832,147
LARP1	154,712,902-154,817,607	58,009,064-58,062,034
CNOT8	154,858,249-154,875,456	58,104,153-58,118,594
GEMIN5	154,887,416-154,938,209	58,120,001-58,168,539
MRPL22	154,941,070-154,969,411	58,171,654-58,179,580

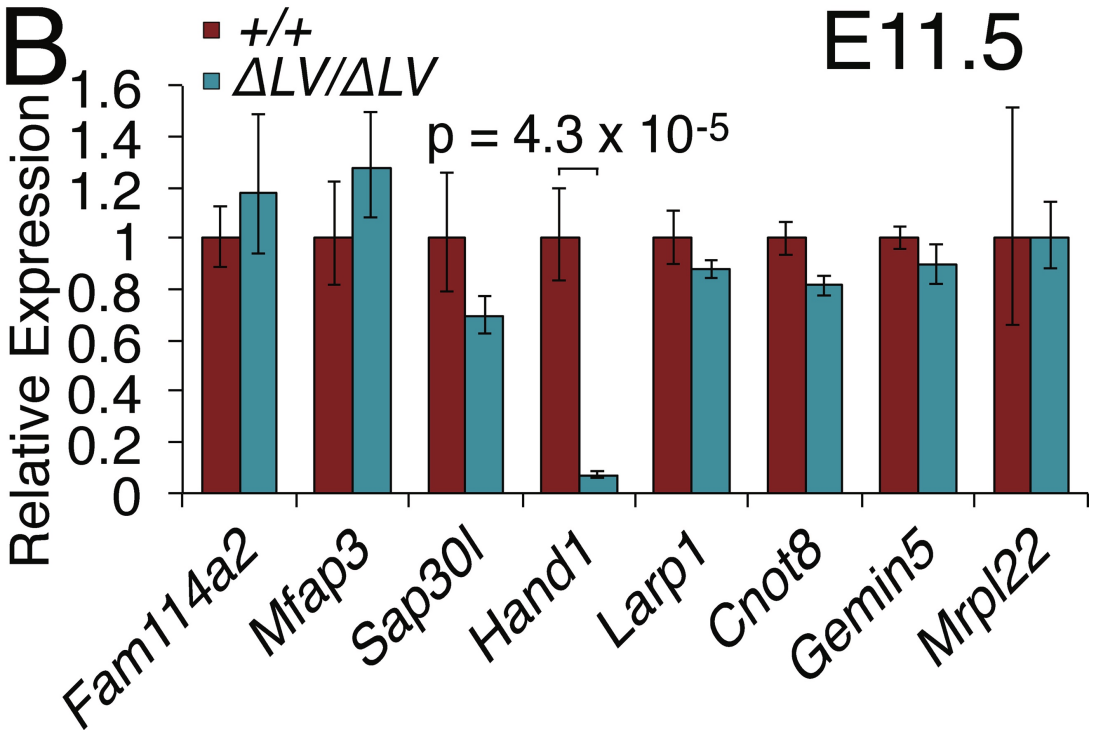

Online Figure II. Within the embryonic ventricle, the *Hand1*^{LV} enhancer is necessary for expression of *Hand1* and no other neighboring genes. A) The positions of genes located within 0.5 Mb 5' and 0.5 Mb 3' of *HAND1* that are evolutionarily conserved between humans and mice are listed. B) qRT-PCR of isolated E11.5 ventricles reveal reduced *Hand1* expression in

Hand1$^{\Delta LV/\Delta LV}$ mutants (n = 6) compared to wild-type controls (n = 4). Expression of neighboring genes is not significantly affected. Expression of *Galnt10* [shaded in (A)] was not detectable in E11.5 ventricles. Asterisks denote significant ($p \leq 0.05$ according to Benjamini-Hochberg false discovery rate) changes in mRNA levels.

Online Figure III.

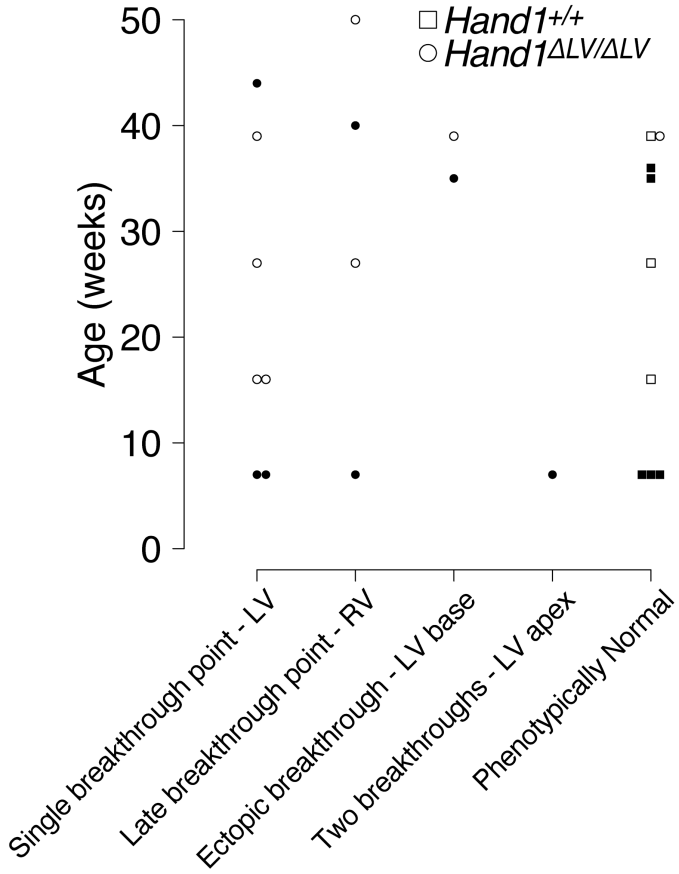

Online Figure III. Epicardial activation phenotypes in *Hand1*$^{\Delta LV/\Delta LV}$ enhancer mutants do not show correlation with age or sex. Epicardial activation phenotypes for *Hand1*$^{\Delta LV/\Delta LV}$ mutants (circles) and *Hand1*$^{+/+}$ littermates (squares) are plotted against age (in weeks). Males and females are represented by open and shaded points, respectively.

Online Figure IV.

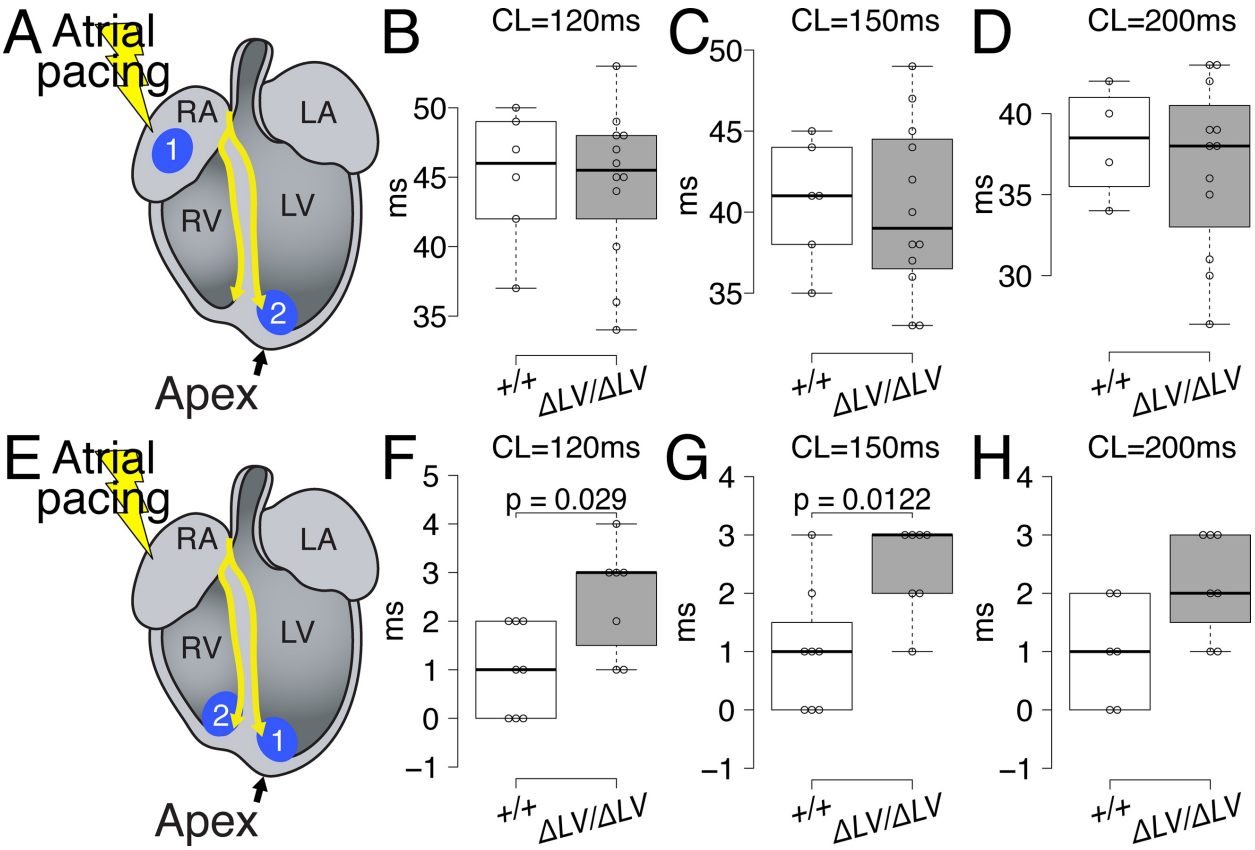

Online Figure IV. RBB activation is delayed in *Hand1*$^{\Delta LV/\Delta LV}$ mutants. A) Schematized atrial pacing illustrates sites (blue dots) corresponding to right atrium (RA; 1) and LV (2) breakthroughs. B-D) LV epicardial breakthroughs, relative to the RA, are not delayed in *Hand1*$^{\Delta LV/\Delta LV}$ (n = 12) relative to *Hand1*$^{+/+}$ (n = 6) hearts at cycle lengths of 120 ms (B), 150 ms (C), or 200 ms (D). E) Schematized atrial pacing illustrates sites (blue dots) corresponding to LV (1) and RV (2) breakthroughs. (B-D) RV epicardial breakthroughs, relative to the LV, are significantly delayed in *Hand1*$^{\Delta LV/\Delta LV}$ (n = 8) relative to *Hand1*$^{+/+}$ (n = 7) hearts at cycle lengths of 120 ms, p=0.029 (F), 150 ms, p=0.0122 (G), or 200 ms p=0.073 (H). Significance determined by Mann-Whitney U test. For box blots, center lines - medians; box limits - 25th and 75th percentiles; whiskers - 1.5X the

interquartile range from the box limits. Individual data points are represented by open circles outliers represented by closed circles.

Online Figure V.

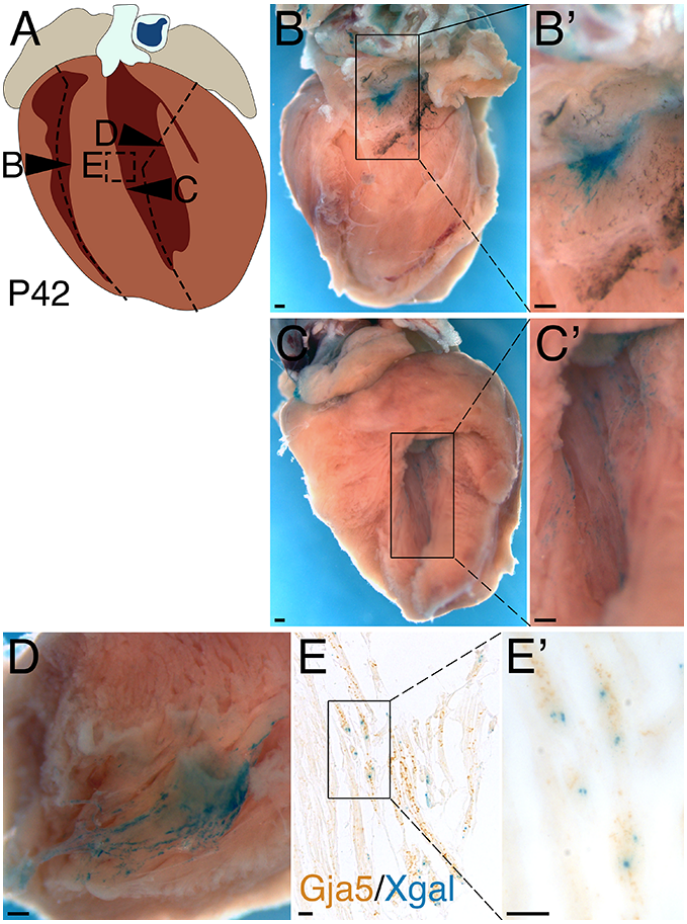

Online Figure V. *Hand1* is expressed in the adult VCS. A) Schematic representation of a P42 heart illustrating planes of dissection, and the resulting views of the ventricular walls shown in panels B-D. B-D) Whole mount preparations of P42 *Hand1*$^{+/lacZ}$ hearts show X-gal staining in the base of the RV septum (B), along the wall of the LV septum (C), and surrounding the papillary muscle connecting with the free wall of the LV (D). B' and C' show high magnification images of the insets in B and C, respectively. Scale bars = 200 μM. (E) Section immunohistochemistry on X-gal-stained P42 hearts show co-localization of GJA5 (brown) and *Hand1*^{lacZ} (blue). Scale bars in E and E' = 20 μM

Online Figure VI.

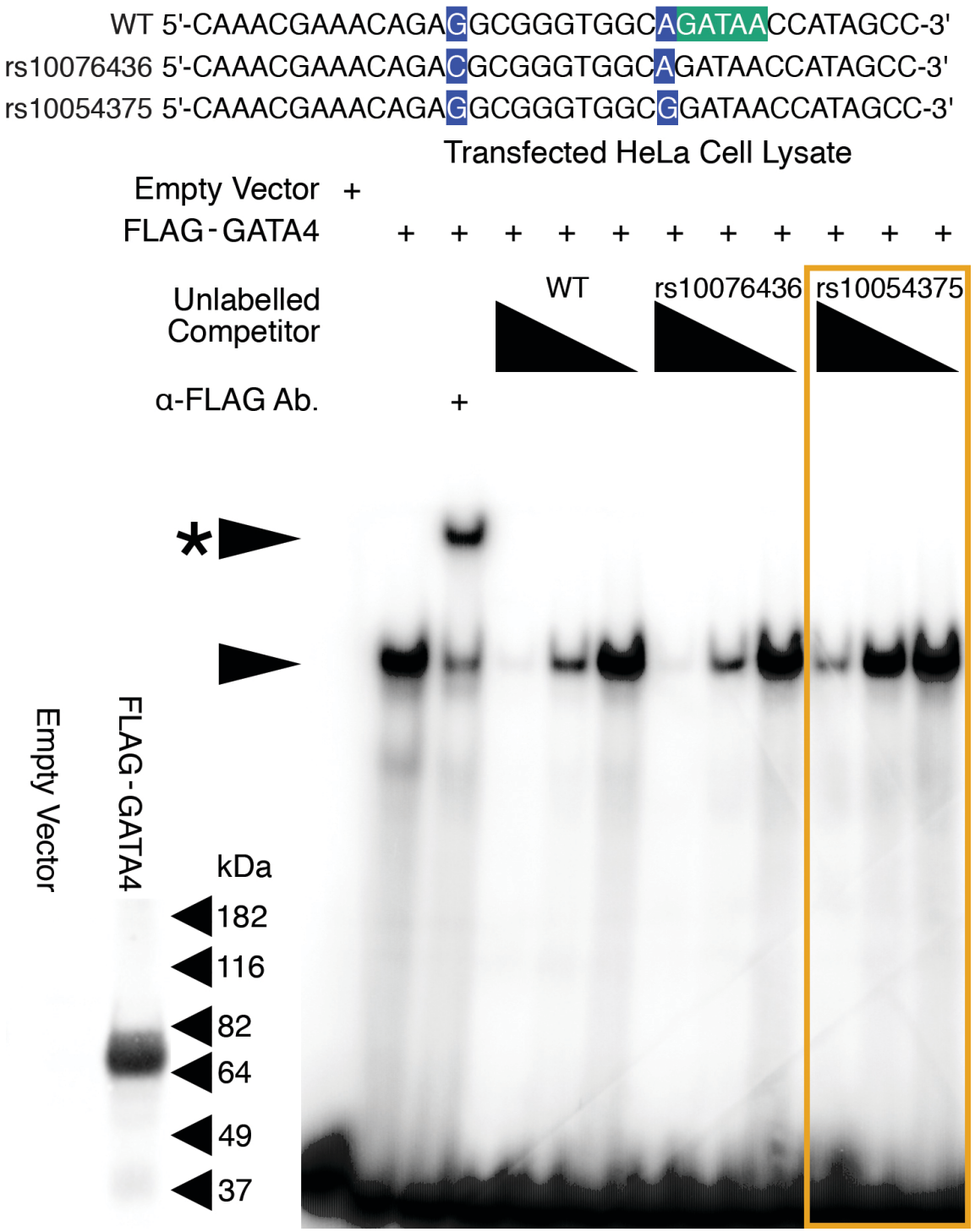

Online Figure VI. GATA4 binding to evolutionarily conserved *cis*-element within the minimal *Hand1* LV enhancer, which is necessary for *Hand1*-reporter *trans*-activation *in vivo*,

is inhibited by a QRS-associated SNP. EMSA using lysates of HeLa cells transfected with FLAG-GATA4 demonstrates Gata4 binding to radiolabeled oligonucleotides mimicking the two GATA consensus sites (GATA 5' and GATA 3') in the *Hand1* LV enhancer. Western blots for α-FLAG (inset) verifies synthesis of FLAG-GATA4. Competition with increasing concentration of unlabeled competitors reveals that the oligo mimicking the minor variant of SNP rs10054375 (boxed in orange) competes less effectively.

Online Figure VII.

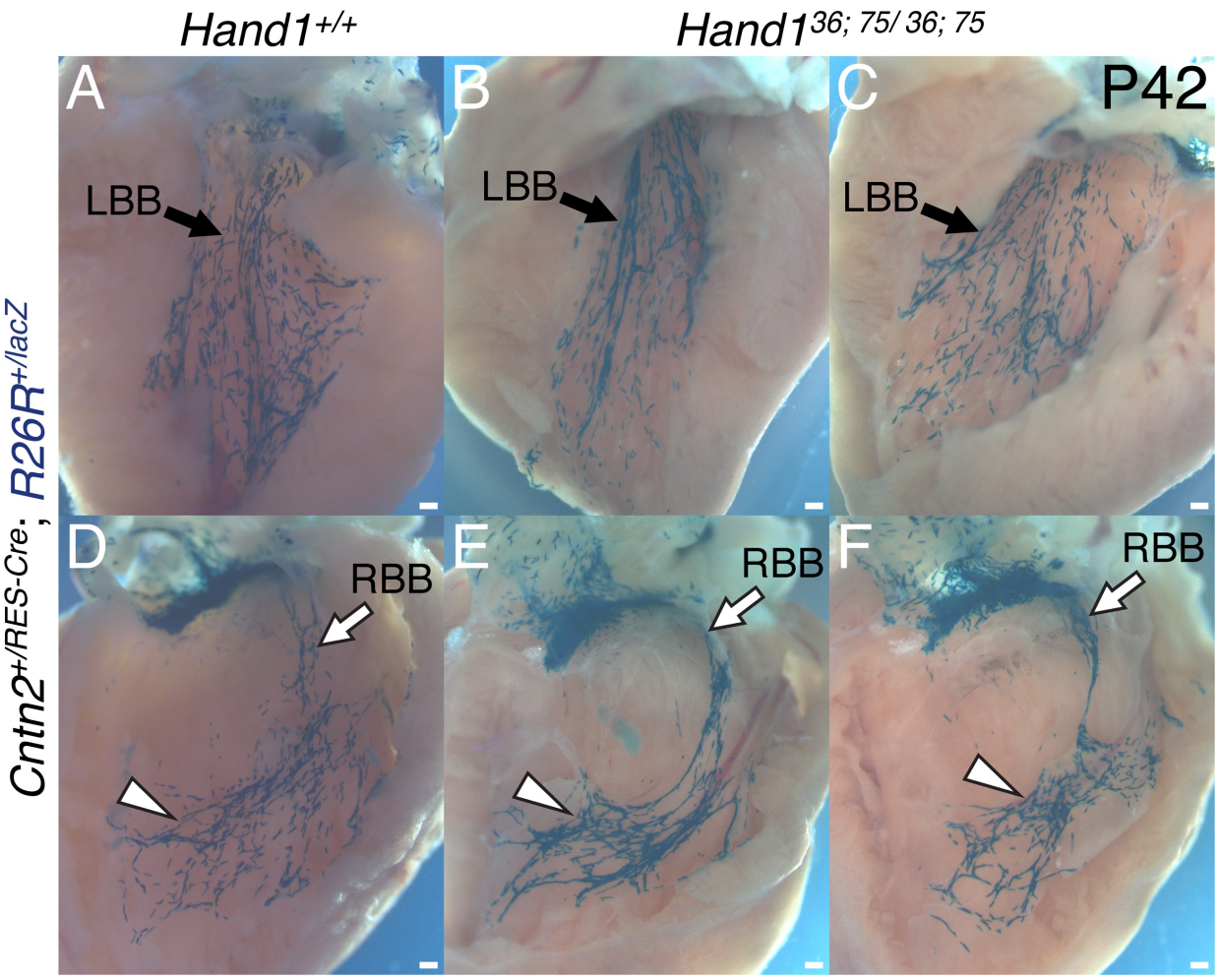

Online Figure VII. *Hand1*$^{36;75/36;75}$ mutants do not display gross abnormalities of the VCS. A-F) P42, X-gal-stained *Hand1*$^{36;75/36;75}$;*Cntn2*$^{+/IRES\text{-}Cre}$;*R26R*$^{+/lacZ}$ hearts (B, C, E, and F) display LBBs (arrows), RBBs (white arrows), and peripheral RBB networks (white arrowheads) that are grossly comparable to *Hand1*$^{+/+}$;*Cntn2*$^{+/IRES\text{-}Cre}$;*R26R*$^{+/lacZ}$ controls (A, D). Scale bars = 200 µM.

Online Table I.

Genotype	Expected	Recovered
+/+	66	71
Hand1$^{\Delta LV/+}$	133	114
Hand1$^{\Delta LV/\Delta LV}$	66	80

n = 265. The chi-square statistic is 2.9865. The p-value is 0.224643. The result is not significant at $p < 0.05$

+/+	25.75	31
Hand1$^{\Delta LV/+}$	25.75	26
Hand1$^{+/lacZ}$	25.75	26
Hand1$^{\Delta LV/lacZ}$	25.75	20

n = 103. The chi-square statistic is 1.2164. The p-value is 0.749073. The result is not significant at $p < 0.05$

Online Table I. Expected and actual survival data of intercrosses of *Hand1*$^{\Delta LV/+}$ mice.

Online Table II.

lead	*Hand1* genotype	n	RR, ms	PQ, ms	QRS1, ms	QRS2, ms	QT, ms
I	*+/+*	20	132.55 ± 4.41	27.71 ± 0.57	7.81 ± 0.23	10.25 ± 0.33	49.22 ± 1.55
	ΔLV/+	19	125.32 ± 5.35	27.59 ± 0.41	7.96 ± 0.21	10.15 ± 0.30	44.81 ± 1.80
	ΔLV/ΔLV	25	136.84 ± 4.38	26.33 ± 0.53	7.89 ± 0.27	10.54 ± 0.34	49.43 ± 1.31
II	*+/+*	20	134.00 ± 3.89	28.41 ± 0.54	7.03 ± 0.18	8.82 ± 0.29	46.22 ± 1.34
	ΔLV/+	19	134.26 ± 4.85	27.83 ± 0.42	7.23 ± 0.27	9.29 ± 0.34	47.07 ± 1.39
	ΔLV/ΔLV	25	142.12 ± 2.89	26.62 ± 0.38	7.60 ± 0.22	10.28 ± 0.23*, #	47.10 ± 1.11
III	*+/+*	20	134.25 ± 3.39	27.98 ± 0.61	8.04 ± 0.24	9.59 ± 0.36	47.41 ± 1.58
	ΔLV/+	19	135.74 ± 4.18	27.29 ± 0.39	8.39 ± 0.26	10.89 ± 0.34	47.08 ± 2.24
	ΔLV/ΔLV	25	142.80 ± 2.75	26.24 ± 0.33&	8.26 ± 0.35	11.14 ± 0.48$	50.54 ± 1.38
I	*+/+*	17	140.65 ± 4.52	28.21 ± 0.65	7.38 ± 0.22	9.33 ± 0.26	47.69 ± 1.18
	+/36; 75	27	141.56 ± 3.98	28.21 ± 0.34	7.38 ± 0.20	9.26 ± 0.26	46.74 ± 1.11
	36; 75/36; 75	32	138.09 ± 5.69	28.46 ± 0.32	7.51 ± 0.18	9.68 ± 0.26	45.92 ± 1.49
II	*+/+*	17	144.47 ± 4.79	28.92 ± 0.57	6.54 ± 0.16	8.12 ± 0.19	40.87 ± 1.01
	+/36; 75	27	144.44 ± 4.16	28.41 ± 0.52	6.64 ± 0.10	8.27 ± 0.14	43.88 ± 0.91
	36; 75/36; 75	32	142.63 ± 4.74	28.77 ± 0.37	6.95 ± 0.12	8.63 ± 0.19	42.52 ± 0.82
III	*+/+*	17	147.29 ± 4.88	28.25 ± 0.61	7.72 ± 0.40	10.56 ± 0.62	48.60 ± 1.78
	+/36; 75	27	147.04 ± 4.08	28.10 ± 0.50	7.77 ± 0.36	9.83 ± 0.57	47.20 ± 1.18
	36; 75/36; 75	32	146.28 ± 4.76	28.30 ± 0.33	8.03 ± 0.25	10.27 ± 0.40	46.52 ± 1.10

*, p = 0.001 vs. *+/+*
#, p = 0.021 vs. *ΔLV/+*
$, p = 0.01 vs. *+/+*
&, p = 0.041 vs. *+/+*
Shaded values are not normally distributed.

Online Table II. ECG analyses of *Hand1* mutants.

Online Movies Legend

Mov. #	Genotype	Pacing	Phenotype
1	*Hand1*$^{+/+}$	Atrial	Phenotypically Normal
2	*Hand1*$^{\Delta LV/\Delta LV}$	Atrial	Single breakthrough point in the LV
3	*Hand1*$^{\Delta LV/\Delta LV}$	Atrial	Late breakthrough point in the RV
4	*Hand1*$^{\Delta LV/\Delta LV}$	Atrial	Ectopic breakthrough proximal to the base of the LV
5	*Hand1*$^{\Delta LV/\Delta LV}$	Atrial	Two breakthroughs proximal to the apex of the LV
6	*Hand1*$^{+/+}$	Apical	Phenotypically Normal
7	*Hand1*$^{\Delta LV/\Delta LV}$	Apical	Phenotypically Normal
8	*Hand1*$^{36;\ 75/36;75}$	Atrial	Single breakthrough point in the RV
9	*Hand1*$^{36;\ 75/36;75}$	Atrial	Two breakthroughs proximal to the apex of the LV
10	*Hand1*$^{+/+}$	Atrial	Phenotypically Normal
11	*Hand1*$^{36;\ 75/36;75}$	Apical	Phenotypically Normal
12	*Hand1*$^{+/+}$	Apical	Phenotypically Normal
13	*Hand1*$^{36;\ 75/36;75}$	Atrial	Single breakthrough point in the LV
14	*Hand1*$^{36;\ 75/36;75}$	Atrial	Two breakthrough points in the LV
15	*Hand1*$^{36;\ 75/36;75}$	Atrial	Late breakthrough point in the RV
16	*Hand1*$^{36;\ 75/36;75}$	Atrial	Diffuse RV breakthrough misplaced toward base
17	*Hand1*$^{36;\ 75/36;75}$	Atrial	Two breakthroughs in the RV - one proximal to the apex and one diffuse and displaced toward the base